Easily Deployable Underwater Acoustic Navigation System for Multi-Vehicle Environmental Sampling Applications

Anwar Quraishi*, Alexander Bahr**, Felix Schill**, Alcherio Martinoli*

***Abstract*— Water as a medium poses a number of challenges for robots, limiting the progress of research in underwater robotics vis-à-vis ground or aerial robotics. The primary challenges are satellite based positioning and radio communication being unusable due to high attenuation of electromagnetic waves in water. We have developed miniature, agile, easy to carry and deploy Autonomous Underwater Vehicles (AUVs) equipped with a suite of sensors for underwater environmental sensing. We previously demonstrated adaptive sampling and feature tracking, and gathered data from a lake for limnological research, with the AUV performing inertial navigation. In this paper, we demonstrate a new underwater acoustic positioning system, which allows on-board estimation of AUV position. Our system uses absolute time information from GNSS for initial clock synchronization and uses one-way-travel-time for range measurements, which makes it scalable in the number of robots. It is easily deployable and does not rely on any installed infrastructure in the environment. We describe various hardware and software components of our system, and present results from experiments in Lake Geneva.**

I. Introduction

The opacity of water to electromagnetic waves limits remote sensing for measuring physical or biological parameters below the surface of water bodies. The underwater domain therefore has many applications for autonomous robots carrying in-situ sensing payloads to capture spatio-temporal phenomena. Not only does the use of robots scale better than static sensing nodes in terms of spatial coverage [1], but robots can also specifically target regions of higher interest for gathering data [2], [3], [1]. However, underwater environments pose a number of challenges, including unavailability of satellite-based positioning. Further, water bodies have few visually distinct features away from the bottom and the water is often turbid, making it difficult or even impossible to rely on vision as a navigation aid. We previously presented our work on autonomous feature tracing and adaptive sampling in a lake with an Autonomous Underwater Vehicle (AUV), for gathering dense limnological measurements from specific regions of interest [4]. The AUV had no external position reference (except for a depth sensor) for underwater localization, and essentially performed inertial navigation. In this paper, we present an acoustic localization system to aid such data gathering missions. An accurate on-board position estimation enables the AUV to accurately follow a pre-planned trajectory. It also provides an accurate geo-reference for each environmental measurement, improving the quality of the data collected by the AUV.

Fig. 1: The Vertex AUV with its sensor suite in the front, protected by a white cage. The AUV is about 70 cm long, weighs 7 kg, and can be carried and deployed easily by one person.

For our work, we used the Vertex AUV [5], shown in Fig. 1, a platform developed in our laboratory and currently manufactured and commercialized by Hydromea S.A.[1]. It is small enough to be easily deployed and retrieved by one person, and was designed for distributed, cooperative multi-AUV sensing. In contrast with many large size commercial AUVs, its small size makes it suitable for deployment in lakes, where large ships with cranes are generally not available. Yet, its small size (0.7 m in length) also introduces further challenges. Commercially available navigation hardware such as a SONAR or a Doppler Velocity Log (DVL) are not only expensive, but are also incompatible with the Vertex AUV due to their size.

A number of approaches that use acoustic signals transmitted by a beacon for computing range or bearing have been proposed for AUV navigation. Knowing the position of multiple transmitting beacons, it is possible to triangulate the position of the AUV [6]. For the case where the beacon locations are not known (but they are known to be fixed), an approach similar to Simultaneous Localization and Mapping (SLAM) can be used, where the beacons and the AUV are simultaneously localized [7]. Becker et al. [8] propose a similar approach using bearing-only measurements from a single beacon with known depth but unknown position. This approach requires multiple receivers to estimate bearing from time difference of arrival at the receivers. If acoustic communication is available, the beacons can transmit their own position. Munafò et al. in [9] encode transmission time information within the signal used for computing range and bearing. Their method relaxes the need for synchronized

* Distributed Intelligent Systems and Algorithms Laboratory (DISAL), School of Architecture, Civil and Environmental Engineering, École Polytechnique Fédérale de Lausanne (EPFL), 1015 Lausanne, Switzerland.
** Hydromea S.A., Lausanne, Switzerland.
This work was funded by the Swiss National Science Foundation under grant CRSII2_160726/1. https://disal.epfl.ch/research/AUVDistributedSensing.

[1] http://www.hydromea.com

clocks or two-way signal exchange for calculating range. This approach relies on beacons being already installed, doing which can be expensive and time consuming. Other methods include matching measured geophysical properties to apriori maps [10], and SLAM-like approaches using a SONAR [11] or vision [12]. They either need apriori information about the environment or require expensive and large equipment such as a SONAR, which cannot be integrated with a miniature AUV. Further, visual SLAM based methods work only in clear, shallow water or close to the bottom. Other approaches to underwater navigation exist that do not rely on acoustic beacon systems or SONAR. Hegrenaes et al. in [13] use a Doppler velocity log (DVL) water-track measurements together with sea current estimates for improved mid-water (away from bottom or surface) navigation. Song et al. also use a similar method, with local current measurements with an acoustic Doppler current profiler (ADCP) combined with ocean current maps preloaded onto an AUV [14].

More recently, Rypkema et al. [15] presented a localization system that uses an Ultra-Short Base Line (USBL) receiver array mounted on an AUV and a single acoustic transmitter. Their approach is similar to the one proposed by us, in that it uses one-way travel time for ranging. On the Vertex AUV, the environmental sensing payload is mounted in the front of the AUV as shown in Fig. 1, in order to prevent the thrusters from disturbing the medium before a measurement is taken. This leaves limited space for installing a USBL array for range-and-bearing measurements.

We propose an acoustic ranging based navigation system that consists of surface-side and AUV-side acoustic transceiver devices. Both use similar hardware but the surface-side devices are additionally equipped with a radio and satellite positioning receivers and are deployed either close to the shore or off-shore. Both kinds of transceiver devices can send and receive acoustic signals, and calculate the range to a transmitter based on time-of-flight of sound in water. However, in this experiment, we use the surface devices exclusively as transmitting beacons, and the AUVs as passive receivers. The proposed system is easy to deploy, does not require any installed hardware in the environment, which will allow us to rapidly set up environmental sampling missions in new environments. The system is scalable in the number of robots, making it suitable for multi-AUV operations. Additionally, we do not rely on expensive clocks (such as chip scale atomic clocks) for time synchronization, but instead use inexpensive crystal oscillators coupled with timing information from the Global Navigation Satellite System (GNSS) receivers.

We introduce the relevant AUV subsystems and other equipment used in our system in Section II. In the following Section (III), we present our approach towards developing and deploying the acoustic navigation system. We show results gathered with real-world experiments in Section IV. Finally, we highlight the importance of acoustic navigation for underwater sampling applications and discuss possibilities for improving the proposed system.

(a) AUV acoustic system (b) Surface beacon

Fig. 2: Acoustic transceivers used on surface and on the AUV. In this paper, we use the surface transceivers exclusively as beacons and AUV transceiver as a passive receiver.

II. Relevant equipment and AUV subsystems

A. On-board Navigation

An Extended Kalman Filter (EKF) framework is used for navigation, which fuses sensor measurements with a comprehensive model of the dynamics of the AUV. The dynamics model takes into account the rotational speed of the propellers, inertia of the AUV, as well as the effect of buoyancy and viscous drag on the body of the AUV. The EKF is complemented by a GNSS position fix whenever the AUV is on the surface. In the absence of any external positioning reference, the AUV is effectively performing dead reckoning, aided by the compass for its heading, an Inertial Measurement Unit (IMU) for attitude, a dynamic model for velocity, and a depth sensor. However, with dead reckoning, the error in the estimated position can increase without bound. Range measurements from the acoustic system can be integrated into the position estimate within the EKF framework, which will help bound the position error.

Acoustic range measurements are subject to multi-path reflections, echoes and noise in the hydrophone signal itself. Clearly, the error in range measurements cannot be accurately modeled with a Gaussian distribution. Therefore, performing an acoustic range update within an EKF framework is not appropriate on a theoretical level because it inherently assumes a Gaussian error model. Despite that, it works well in practice and offers a number of advantages such as low computational cost and simple implementation, which make it suitable for a real-time system.

B. AUV acoustic subsystem

The acoustic subsystem consists of two piezoelectric transducers, one for transmitting an acoustic signal and the other that acts as an acoustic receiver. These transducers are respectively connected to the digital-to-analog and analog-to-digital converter modules of a microcontroller with appropriate amplification stages. The microcontroller samples the acoustic signal, measures the time of flight and computes the range, and transmits this information to the navigation module over a serial link. All the electronics and the transducers are molded into a separate waterproof and pressure-proof casing which is attached to the AUV hull, as shown in Fig. 2a. In this paper, we only use the receiving transducer, and the AUVs do not transmit any acoustic signal.

Fig. 3: An ASV, which can carry the surface beacons or serve as surrogates for the AUVs for various experiments.

C. Surface beacons

The surface acoustic devices, shown in Fig. 2b have similar hardware as the acoustic subsystem on the AUV described in the previous section, except that they are additionally equipped with their own GNSS receiver and a radio module for communication with the base station. They also have multi-channel input for connecting to a hydrophone array, for future implementation of bearing-based tracking methods (which will require AUVs to be transmitting). These devices can be deployed from the shore, or mounted on a surface vehicle or a boat and deployed at any point in a water body. For the experiments described in this paper, we use them as beacons that transmit an acoustic signal. They do not receive any signal since the AUV is not transmitting.

D. Autonomous surface vehicles

We have a number of small, lightweight (about 1 m in length and 1 kg in weight) Autonomous Surface Vehicles (ASVs), shown in Fig. 3, which are remote-controlled boats outfitted with an autopilot. The surface acoustic beacons are mounted on these vehicles for off-shore deployment, with the acoustic transceivers and the autopilot sharing the radio and GNSS receiver modules. Due to wind and waves, it is difficult to deploy static but unanchored off-shore beacons. The ASVs instead can actively hold a specified position, so that the AUVs can receive acoustic pings from beacons at known locations. Future implementation of acoustic-based communication will enable the beacons to broadcast their position, eliminating the need for keeping the beacons static.

The ASVs can also follow a pre-planned trajectory, and can be used as surrogates for AUVs for testing and experimentation.

III. Methodology

A. Surface beacon deployment

We deployed one beacon from the shore in Lake Geneva, and another mounted on an ASV, as shown schematically in Fig. 4. The ASV was programmed to hold a specific position. Once the beacons are deployed, their positions are transmitted to the AUV before it dives. Since the AUV is equipped with a depth sensor, position estimation reduces to a two-dimensional problem. Given that the initial position of the AUV is known from GNSS before launch and incremental inertial updates are available, in most benign configurations, two beacons are sufficient to fully estimate the AUV position. We can tune the accuracy of the system by altering the relative location of the two (or more) beacons.

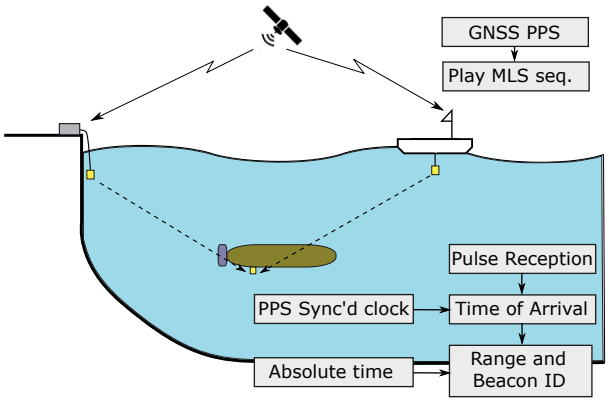

Fig. 4: One beacon is deployed from the shore and another mounted on an ASV. The two surface beacons transmit alternatively following a fixed schedule based on absolute time, and use the GNSS PPS to trigger playback of an acoustic pulse. The AUV uses absolute time to identify the current transmitter and computes time of flight.

B. Clock and time synchronization

For computing range from one-way travel time and for scheduling transmissions from multiple beacons, we need all the beacons and the AUV to have synchronized clocks. We do that at two levels. First, we use the timing pulse emitted per second (PPS) by the Ublox M8N GNSS receiver module, which has an accuracy of the order of 10 ns, to tune the *speed* of the clock and eliminate the clock drift. This helps in accurate measurement of time of arrival of the ranging pulse, as explained in the next section. Second, we use the absolute time information received from the GNSS module to set the wall-clock time. The absolute time solution has an error of the order of 10 ms. To mitigate that, we first set the wall-clock time to the GNSS time solution, and then round it off to the next full second at the PPS trigger. With a known transmission schedule and synchronized clocks, each device knows the identity of the current and previous transmitter.

The AUV clock is synchronized while it is on surface, but the clock drifts when underwater. For this reason, the AUV is equipped with an crystal oscillator of higher accuracy and temperature compensation. It has a clock drift of 0.3 ppm, which translates to a range measurement error of less than 1 m over 1 hour. This error is insignificant compared to the accumulated error in purely inertial positioning. Nonetheless, this clock drift can be reset with GNSS reception during the periodic resurfacing of the AUV.

C. One-way travel time and transmission scheduling

Our system is based on one-way travel time for ranging, where only the surface beacons transmit and the AUVs are passive receivers. This has the advantage of scalability, since any number of AUVs can receive the ranging pulse transmitted by a beacon. We use the PPS signal, which is fed to an interrupt pin, to trigger playback of a pre-recorded

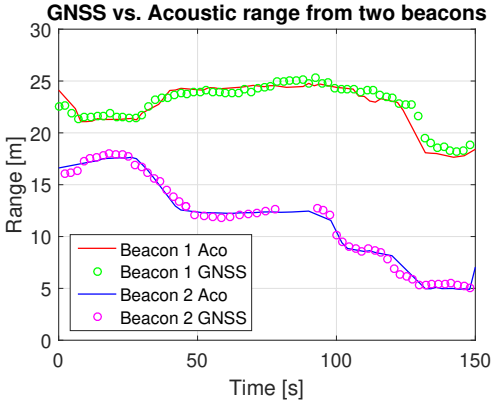

Fig. 5: Range measured using one-way travel time by a receiver to two beacons that transmit according to a prearranged schedule. Range computed by GNSS positions is shown for comparison. The receiver associates each range measurement to the correct transmitter beacon using absolute time information from GNSS.

maximum length sequence (MLS) pulse through the beacon transducer. The receiver then measures the time between its own PPS trigger and the acoustic pulse reception to compute time of flight. We assume constant velocity of sound in the region of operation during the length of the experiment.

Since only one of the surface beacons can transmit at a time in order to avoid interference, we need to schedule their transmission. We use the PPS signal to trigger the transmission on either of the two beacons every full second of the clock. While this places a maximum limit on the range that can be measured by our system, it can be increased if necessary by altering the transmission schedule. We schedule the transmissions for each beacon based on absolute time, and this schedule is known to all devices prior to a mission. Fig. 5 shows that the receiver can correctly identify the transmitting beacon for each range measurement.

D. Position updates with acoustic range

We integrate the acoustic range measurements with the AUV position within the existing EKF framework. In two dimensions, given the prior position of the AUV, $\hat{\vec{x}}$ and covariance $\hat{\Sigma}$, and a beacon located at position $\mathbf{x}_{\text{beacon}}$, our measurement function is

$$h(\mathbf{x}) = \|\mathbf{x} - \mathbf{x}_{\text{beacon}}\|. \tag{1}$$

On receiving a range measurement r, the posterior position and covariance is obtained using the regular Kalman update equations,

$$\vec{x} = \hat{\vec{x}} + K_{\text{gain}}(r - h(\hat{\vec{x}})), \tag{2}$$

$$\Sigma = (\mathbf{I} - K_{\text{gain}}\mathrm{H})\hat{\Sigma}, \tag{3}$$

where H is the Jacobian of $h(\mathbf{x})$, and the Kalman gain is computed as

$$K_{\text{gain}} = \hat{\Sigma}\mathrm{H}^{\mathrm{T}}\left[\mathrm{H}\hat{\Sigma}\mathrm{H}^{\mathrm{T}} + \sigma_r\right]^{-1}. \tag{4}$$

Note that the bracketed expression is a scalar and hence there is no matrix inversion involved, which makes this update computationally inexpensive.

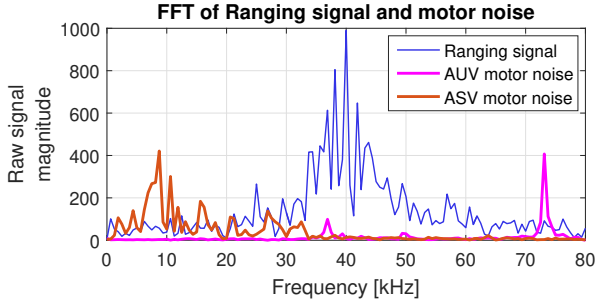

Fig. 6: FFT of the ranging signal and the motor-induced noise of AUV and ASVs. The ranging signal is a pre-recorded MLS sequence that is sent through a piezo, which has resonance in the 35-45 kHz range.

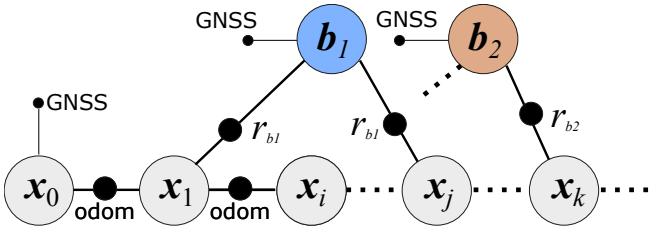

Fig. 7: Factor graph for smoothing the trajectory estimated by EKF, which fuses odometry and acoustic range measurements. x_n are vehicle positions, connected in a chain by odometry factors. b_1 and b_2 are beacon positions, which are connected to vehicle positions by range measurement factors.

E. Signal filtering and outlier rejection

The mechanical noise of the motors is also picked up by the acoustic receiver, which generates spurious range measurements. A Fourier transform of the motor noise shows the presence of frequencies beyond the 70 kHz range for the AUV, and sub 30 kHz range for ASVs. While we use an MLS signal as the ranging pulse which contains a wide range of frequencies, the transmitters have a resonance in the 35-45 kHz range. Therefore, the ranging pulse is band-limited. A band pass filter with a lower and upper cut-off frequencies of 30 kHz and 50 kHz respectively effectively removes the motor induced disturbance.

Echoes and reflected signal arrivals result in outlier range measurements. These errors are exacerbated especially when operating in shallow water bodies or close to the shore, as is the case for the experiments presented in this paper. Using the dynamics model of the AUV combined with the past range measurements, such outliers can be rejected. More specifically, using the current position estimate (which is a function of the dynamics model) and the range measurement model, a likelihood function for range measurements is formulated. Then, range measurements with likelihood less than a set threshold are classified as outliers. Usually, outliers with a large error are easily rejected since they have a low likelihood. However, occasional outliers with small errors may be difficult or even impossible to eliminate.

F. Post-processing

While the EKF is computationally efficient for on-board fusion of acoustic range measurements, each update is performed by marginalizing out the previous state estimates and measurements. This sometimes results in discontinuities in the estimated trajectory when acoustic range updates are

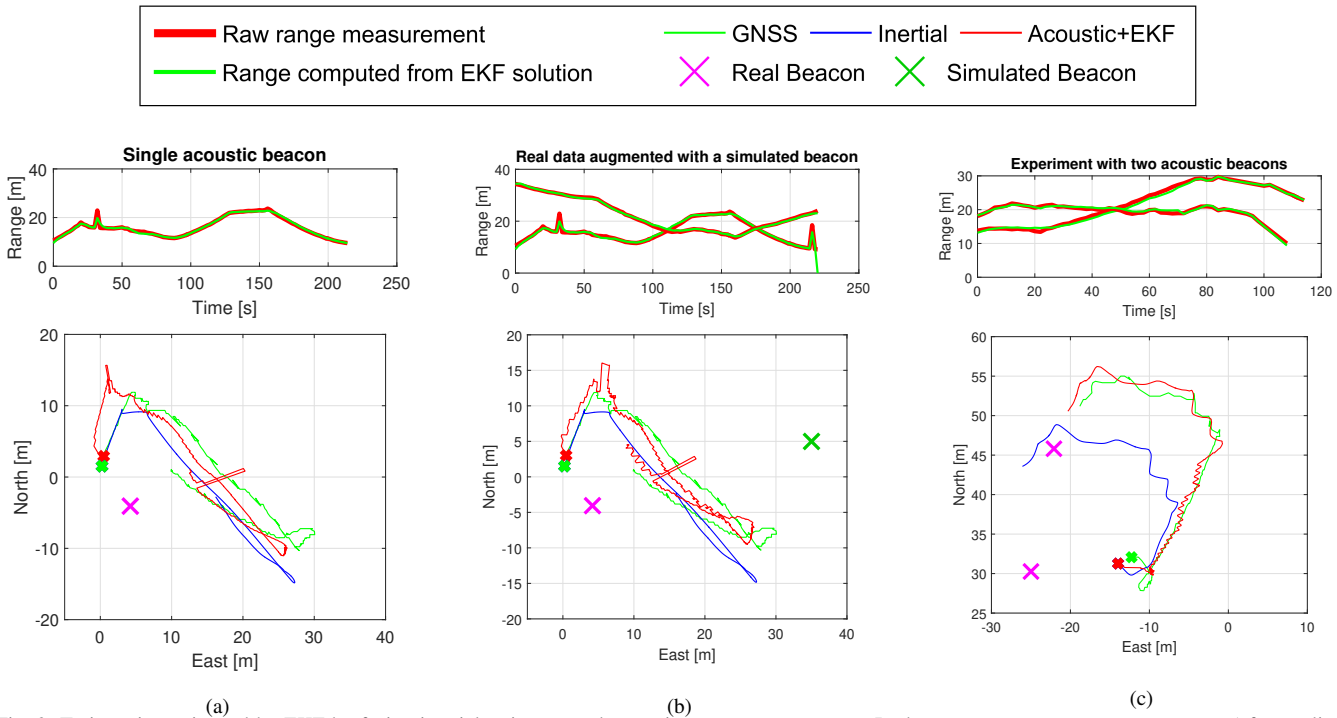

(a) (b) (c)

Fig. 9: Trajectories estimated by EKF by fusing inertial estimates and acoustic range measurements. In the top row, raw range measurements (after outlier rejection) are compared with range computed from the EKF solution. Plot (a) shows an experiment with a single beacon. The colored crosses on the plot indicate the starting point of the mission. In (b), a virtual beacon with simulated range measurements is added to the data logged during the mission in (a). This helps in experimenting with beacon placement and studying its impact on navigation accuracy. (c) shows an experiment with two beacons, the range measurements from which are used by a receiving vehicle to perform online real-time position estimation. Ground truth trajectory obtained from GNSS is shown in all the three plots.

performed with erroneous range measurements. However, in post processing, we can use the odometry information (control inputs and inertial measurements) logged by the vehicle together with the set of all range measurements to optimize over the whole trajectory. To do so, we represent the vehicle positions, odometry updates and range measurements as a factor graph, as shown schematically in Fig. 7. In the factor graph formulation, consecutive vehicle positions are related through *odometry* factors, while external measurements are represented by their respective *measurement* factors. Essentially, a factor graph represents the joint distribution $P(\vec{x}_1, \vec{x}_2, \dots \vec{x}_n | z_1, z_2, \dots)$, where $\vec{x}_i$ are vehicle positions and z_i are any measurements. Our goal is to estimate the collection of vehicle positions over the entire trajectory. We assume that the first position of the vehicle is known from GNSS reception on the surface, and hence is added as a prior constraint. We then perform a Maximum A-Posteriori (MAP) inference over the factor graph using the GTSAM library [16].

IV. Experiments and Results

We performed a number of experiments with one and two surface beacons in a shallow area of Lake Geneva, close to a boat pier. The first beacon was deployed from the shore, and the second was mounted on an ASV and deployed offshore. The ASV was programmed to hold a static position. Errors in localization due to position-holding inaccuracy of the ASV were not accounted for. The depth in the area was between 2-10 m, and the experiments were performed in low wind and current conditions.

In order to be able to use GNSS position as ground-truth for validation of the proposed system, we mounted the acoustic receiver on a second surface vehicle. This ASV served as a proxy for the AUV, and did not use the GNSS position for navigation. It was simultaneously performing inertial position estimation, as well as fusing acoustic range measurements into its inertial estimate using an EKF. The inertial estimates and the EKF output were both logged.

A. Acoustic navigation

To begin with, we deployed a single transmitting beacon emitting a ranging pulse once every 2 s. The estimated trajectory of the robot is shown in Fig. 9a. The quality of the position estimate in this case will depend on the position and direction of motion of the vehicle relative to the beacon. In order to experiment with various placements for the second beacon, we added a virtual beacon and simulated range measurements in post-processing using data from the aforementioned mission. Fig. 9b shows an instance of a simulated beacon experiment. As expected, adding an additional beacon or increasing the relative separation between the beacons improves the position estimate. We use the GNSS positions as ground truth and compute the RMS error in the estimated trajectory. The error for one and two beacons and various relative beacon placements is summarized in Table I. We then deployed two real beacons and repeated the experiment, with the beacons transmitting

Method / Baseline	Trajectory RMS error [m]
Inertial (Fig. 9a and 9b)	4.26
Single beacon (Fig. 9a)	2.90
Real+virtual / 30 m (Fig. 9b)	2.16
Real+virtual / 45 m (plot not shown)	2.00
Real+virtual / 60 m (plot not shown)	1.87
Inertial (Fig. 9c)	6.90
Two beacons / 16 m (Fig. 9c)	2.10

TABLE I: RMS error over the trajectory for purely inertial navigation and acoustic range based navigation. For the case where two beacons are used, the inter-beacon distance is mentioned.

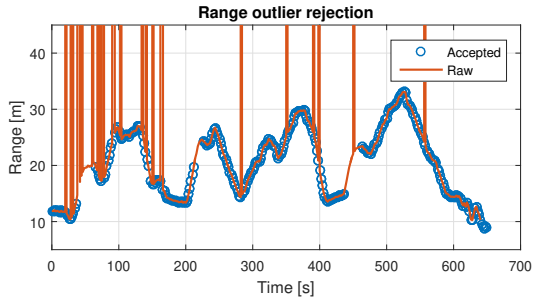

Fig. 10: Raw range measurements with outliers or spurious range measurements (caused by motor noise) and range measurements that are accepted for fusion using EKF.

their ranging pulse every alternate second. Fig. 9c shows the estimated trajectory from this experiment.

B. Outliers and range errors

Fig. 10 shows a plot of raw range measurements and the measurements that were accepted for fusion with the EKF into the position estimate. In practice, outliers with a large error are easily rejected since they have a low likelihood. However, outliers with smaller errors have a larger potential to influence the state estimate. While range measurements help bound the absolute error in the robot trajectory, outlier range measurements result in discontinuities and jumps in the estimated trajectory. There are a number of methods to address these in post-processing.

C. Factor graph smoothing

Offline factor graph smoothing is performed on the estimated trajectory using the GTSAM library, as explained in Section III-F, and the result is shown in Fig. 11. This results in a smooth and consistent trajectory estimate, and therefore provides consistent geo-referencing for data gathered during sampling missions.

V. Conclusion

We presented an acoustic navigation system for AUVs to aid environmental sampling missions in lakes and coastal areas. Our goal was to provide the AUVs with an external positioning reference so as to bound the error in estimated position. This is necessary in order to follow a pre-planned trajectory as well as to correctly geo-reference environmental measurements. The acoustic navigation system presented in this paper is easy to deploy and does not require any

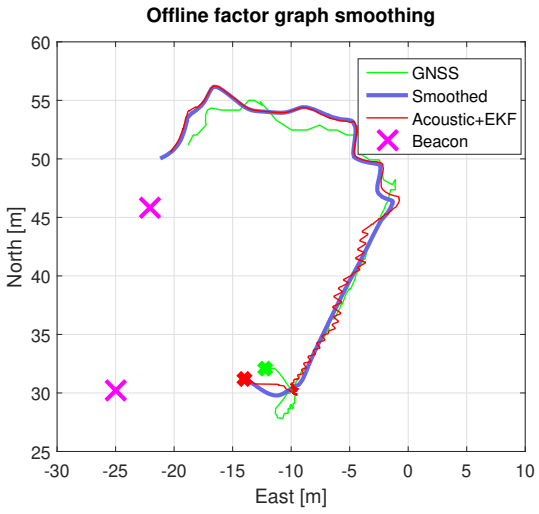

Fig. 11: Factor graph smoothing is applied offline in post processing to the trajectory estimated by EKF.

equipment to be installed in the environment. This is a necessary feature to facilitate quick measurement missions in new environments. Further, our system is scalable in the number of vehicles since the vehicles are passive receivers of acoustic ranging signals. We demonstrated our system with experiments in a real-world environment. The experiments presented in this paper were conducted in shallow water close to the shore of Lake Geneva, which is a challenging environment for acoustic-based localization methods. We used a likelihood-threshold based method to reject outlier range measurements.

A number of improvements to the proposed system are planned in future. Statistical outlier rejection methods are more robust, but they introduce a delay in range updates since they use new range measurements to identify outliers in the past. However, it is possible to perform a delayed correction of the position estimate. We are exploring online, incremental smoothing methods to address the problem of discontinuities and jumps in the estimated trajectory.

References

[1] R. Wang, M. Veloso, and S. Seshan, "Active sensing data collection with autonomous mobile robots," in *IEEE International Conference on Robotics and Automation*, 2016, pp. 2583–2588.

[2] D. E. Soltero, M. Schwager, and D. Rus, "Decentralized path planning for coverage tasks using gradient descent adaptive control," *The International Journal of Robotics Research*, vol. 33, no. 3, pp. 401–425, 2014.

[3] G. A. Hollinger and G. S. Sukhatme, "Sampling-based robotic information gathering algorithms," *The International Journal of Robotics Research*, vol. 33, no. 9, pp. 1271–1287, 2014.

[4] A. Quraishi, A. Bahr, F. Schill, and A. Martinoli, "Autonomous Feature Tracing and Adaptive Sampling in Real-World Underwater Environments," in *IEEE International Conference on Robotics and Automation*, 2018, pp. 5699–5704.

[5] F. S. Schill, A. Bahr, and A. Martinoli, "Vertex: A New Distributed Underwater Robotic Platform for Environmental Monitoring," in *International Symposium on Distributed Autonomous Robotic Systems, 2016*, vol. 6. Springer Proceedings in Advanced Robotics, 2018, pp. 679–693.

[6] J. J. Leonard and A. Bahr, "Autonomous underwater vehicle navigation," in *Springer Handbook of Ocean Engineering*. Cham: Springer International Publishing, 2016, pp. 341–358.
[7] L. Stutters, H. Liu, C. Tiltman, and D. J. Brown, "Navigation technologies for autonomous underwater vehicles," *IEEE Transactions on Systems, Man, and Cybernetics, Part C (Applications and Reviews)*, vol. 38, no. 4, pp. 581–589, 2008.
[8] C. Becker, D. Ribas, and P. Ridao, "Simultaneous sonar beacon localization & AUV navigation," *IFAC Proceedings Volumes*, vol. 45, no. 27, pp. 200–205, 2012.
[9] A. Munafò, T. Furfaro, G. Ferri, and J. Alves, "Supporting AUV localisation through next generation underwater acoustic networks: Results from the field," in *IEEE/RSJ International Conference on Intelligent Robots and Systems*, 2016, pp. 1328–1333.
[10] S. Tuohy, N. Patrikalakis, J. Leonard, J. Bellingham, C. Chryssostomidis *et al.*, "Map based navigation for autonomous underwater vehicles," *International Journal of Offshore and Polar Engineering*, vol. 6, no. 01, 1996.
[11] J. L. Leonard, R. N. Carpenter, and H. J. S. Feder, "Stochastic mapping using forward look sonar," *Robotica*, vol. 19, no. 5, pp. 467–480, 2001.
[12] R. M. Eustice, O. Pizarro, and H. Singh, "Visually augmented navigation for autonomous underwater vehicles," *IEEE Journal of Oceanic Engineering*, vol. 33, no. 2, pp. 103–122, 2008.
[13] O. Hegrenaes and E. Berglund, "Doppler water-track aided inertial navigation for autonomous underwater vehicle," in *OCEANS 2009-EUROPE*, May 2009, pp. 1–10.
[14] Z. Song and K. Mohseni, "Long-term inertial navigation aided by dynamics of flow field features," *IEEE Journal of Oceanic Engineering*, vol. 43, no. 4, pp. 940–954, Oct 2018.
[15] N. R. Rypkema, E. M. Fischell, and H. Schmidt, "One-way travel-time inverted ultra-short baseline localization for low-cost autonomous underwater vehicles," in *IEEE International Conference on Robotics and Automation*, 2017, pp. 4920–4926.
[16] F. Dellaert, "Factor graphs and GTSAM: A hands-on introduction," Georgia Institute of Technology, Tech. Rep., 2012.